Journal of Molecular Catalysis B: Enzymatic 66 (2010) 8–14

Contents lists available at ScienceDirect

Journal of Molecular Catalysis B: Enzymatic

journal homepage: www.elsevier.com/locate/molcatb

Review

Fabrication of a novel glucose biosensor based on Pt nanoparticles-decorated iron oxide-multiwall carbon nanotubes magnetic composite

Jingjing Li, Ruo Yuan*, Yaqin Chai, Xin Che

Key Laboratory on Luminescence and Real-Time Analysis, Ministry of Education, College of Chemistry and Chemical Engineering, Southwest University, Chongqing 400715, China

ARTICLE INFO

Article history:
Received 5 November 2009
Received in revised form 28 February 2010
Accepted 12 March 2010
Available online 20 March 2010

Keywords:
Glucose biosensor
Glucose oxidase
Iron oxide
Multiwall carbon nanotubes
Pt nanoparticles

ABSTRACT

A sensitive and selective amperometric glucose biosensor was obtained by using the electrodeposition of Pt nanoparticles on iron oxide-multiwall carbon nanotubes/chitosan (Fe_yO_x-MWCNTs/CS) magnetic composite modified glassy carbon electrode (GCE) followed by the adsorption of glucose oxidase (GOx) at the surface of the electrode. Fe_yO_x-MWCNTs magnetic composite was characterized by transmission electron microscopy (TEM). The modified process and the electrochemical characteristics of the resulting biosensor were characterized by cyclic voltammetry (CV), electrochemical impedance spectroscopy (EIS), and chronoamperometry. The proposed biosensor exhibit excellent electrocatalytic activity and good response performance to glucose. The influence of various experimental conditions was examined for the determination of the optimum analytical performance. Under the optimal conditions, a linear dependence of the catalytic current upon glucose concentration was obtained in the range of 6.0×10^{-6} to 6.2×10^{-3} M with a detection limit of 2.0×10^{-6} M, and a response time of less than 8 s. The apparent Michaelis–Menten constant (K_M^{app}) was evaluated to be 9.0 mM. Furthermore, the sensitivity for the determination of glucose at the GOx/Pt/Fe_yO_x-MWCNTs/CS magnetic composite modified GCE is better than at common GOx/Pt/MWCNTs/CS and GOx/Pt-Fe_yO_x/CS composite modified electrodes. The proposed biosensor has good anti-interferent ability and long-term storage stability after coating with Nafion, and it can be used for the determination of glucose in synthetic serum.

Contents

* Corresponding author. Tel.: +86 23 68253172; fax: +86 23 68253172.
E-mail address: yuanruo@swu.edu.cn (R. Yuan).

1381-1177/$ – see front matter © 2010 Elsevier B.V. All rights reserved.
doi:10.1016/j.molcatb.2010.03.005

1. Introduction

In recent years, the development of glucose biosensor has been received considerable attention, because determination of glucose concentration is very important in food and fermentation analysis, textile industry, environmental monitoring, medical diagnosis, and many other fields [1,2]. Much effort has been focused on developing suitable techniques for precisely monitoring the glucose level in its biological environment. Those techniques employed for glucose analysis involve a surface plasmon resonance biosensor [3], near-infrared optical biosensor [4], capacitive detection [5], electrochemiluminescene [6], colorimetry [7] and amperometric biosensor, etc. [1,8–10]. Since the development of the first glucose biosensor, much attention has been focused on the improvement of the response performances of enzyme electrodes for biosensor research [11]. Among these sensors, amperometric glucose biosensors have received considerable interest, because this class of technique is characterized by high sensitivity and selectivity, easy operation, compatibility for miniaturization and low cost.

The key step in the development of glucose biosensor is the effective immobilization of GOx on the electrode surface. During recent years, various approaches had been taken to immobilize enzymes onto solid substrates including adsorption, covalent coupling and tethering via an intermediate linker molecule [12,13]. However, most of these biosensors were weak in retaining the bioactivity of GOx and poor in sensitivity. Research for new materials and methods for immobilizing enzyme is still a very important subject to get more active and stable biosensors [14]. Recently, magnetic nanoparticles have attracted increased interest due to its good biocompatibility, strong superparamagnetic, low toxicity, and easy preparation process. The successful applications of magnetic nanoparticles in the immobilization of bimolecular have also been reported [15]. For example, Kaushik et al. have fabricated a glucose biosensor for measuring glucose utilizing CH-Fe_3O_4 magnetic nanocomposite film on which GOx was adsorbed [16]. Cao et al. have reported an electrochemical biosensors utilizing electron transfer in heme proteins immobilized on Fe_3O_4 nanoparticles [17].

On the other hand, it is well known that CNTs have unique structure, high chemical stability and high surface-to-volume ratio, which have been attained considerable attention and have been regarded as a promising candidate for fabricating chemical sensors [18,19]. In particular, recent studies demonstrated the capability of CNTs to promote the electron transfer reactions of enzymatically generated species, such as hydrogen peroxide and p-nitrophenol [20,21]. Actually, several CNTs-based unmediated glucose biosensors have been reported [22,23]. Just recently, the research interest has extended to modify CNTs with other nanomaterials so as to improve dispersity of CNTs in solvents or impart new optical, electric, magnetic properties of CNTs [24,25]. Various CNTs-based composites have been derived from decorating CNTs with metals, metal oxides, and semiconducting nanoparticles [26–28]. More importantly, more and more researches have been conducted towards decorating CNTs with iron oxide and preparing magnetic carbon nanomaterials due to their potential applications in electric device, magnetic data storage and heterogeneous catalysis. Based on the good biocompatibility of Fe_3O_4 MNPs and excellent electrochemical behavior and catalytic property of CNTs, the Tyr/MNPs-CNTs/GCE biosensor showed broad linear responses and high sensitivity for the determination of phenol [29].

In this work, an electrocatalytic enzyme biosensor based on Pt nanoparticles-decorated Fe_yO_x-MWCNTs magnetic composite substrate was developed. The prepared Fe_yO_x-MWCNTs/CS composite possessed high surface area, good mechanical stability, and good conductivity, which provided a compatible microenvironment for maintaining the activity of the immobilized enzyme, and increased the enzyme loading. Furthermore, the Pt nanoparticles were electrodeposited in the MWCNTs-Fe_yO_x magnetic composite in order to improve the electrocatalytic behavior for hydrogen peroxide which is released by the action of GOx upon glucose. The resulting Pt/Fe_yO_x-MWCNTs magnetic material brings new capabilities for electrochemical devices by using the synergistic action of Pt nanoparticles, MWCNTs and Fe_yO_x. Then, the immobilization of GOx onto electrode surfaces was carried out by Pt nanoparticles which has large specific surface area and good biocompatibility. At last, an amperometric glucose biosensor was fabricated by modifying Nafion on the as-prepared electrode. Nafion was coated on the top of the GOx/Pt/Fe_yO_x-MWCNTs/CS composite modified GCE in order to improve the anti-interferent ability and prevent the loss of the GOx. The electrochemical characteristics of the biosensors were described, including the sensitivity, detection limit, linear range, response time, and stability.

2. Experiments

2.1. Reagents and apparatus

Glucose oxidase (E.C 1.1.3.4, 151,000 unit/g) and Chitosan (deacetylating grade: 70–85%) were purchased from Sigma (St. Louis, MO, USA). The multi-walled carbon nanotubes (MWCNTs, >95% purity) were obtained from Chengdu Organic Chemicals Co., Ltd., of the Chinese Academy of Science. Prior to use, MWCNTs were treated with concentrated nitric acid in order to introduce carboxylic acid groups according to report [30]. β-D-glucose and H_2PtCl_6 were bought from Chongqing Chemical Reagent Co. (China). Double distilled water was used throughout this study. Other chemicals and solvents used were of analytical grade and were used as received.

CV measurements were carried out with a CHI 660a electrochemistry workstation (Shanghai CH Instruments, Shanghai, China), with a conventional three-electrode system consisted of a modified GCE as working electrode, a platinum wire as auxiliary electrode, and a saturated calomel electrode (SCE) as reference electrode. All potentials were measured and reported versus the SCE. The morphology and the composition of the Fe_yO_x-MWCNTs were estimated from TEM (H660, Hitachi Instrument Co., Japan). EIS measurements were carried out with a Model (IM6e, ZAHNER elektrik, Germany) and the frequency range is at 100 mHz–10 kHz at 220 mV versus SCE.

2.2. Preparation of Fe_yO_x-MWCNTs magnetic composite

The magnetic composite was prepared according to the literatures [31] with a little modification. In a typical synthesis, the magnetic composite was prepared from a suspension of 0.41 g pretreated MWCNTs in a 75 mL solution of 1.49 g $FeCl_3{\cdot}6H_2O$ and 0.76 g $FeSO_4{\cdot}7H_2O$ at 75 °C under N_2 condition. Then the NaOH solution (30 mL, 0.5 M) was added dropwise into the mixture with vigorously agitation until the pH value reached 11. The mixture was aged at 75 °C for 4 h and was washed three times with doubly distilled water. The obtained sample was dried in an oven at 60 °C for 10 h. The relevant chemical reactions can be expressed as follows:

$$Fe^{2+} + 2Fe^{3+} + 8OH^- + MWCNTs \rightarrow MWCNTs/Fe_3O_4 + 4H_2O \quad (1)$$

$$2Fe^{3+} + 5OH^- + MWCNTs \rightarrow MWCNTs/Fe_2O_3 + 2H_2O + H^+ \quad (2)$$

2.3. Preparation of Fe_yO_x-MWCNTs/CS composite material

Appropriate amount of MWCNTs-Fe_yO_x composite was mixed with 0.2% of CS (0.05 mM acetic acid). The mixture was stirred for

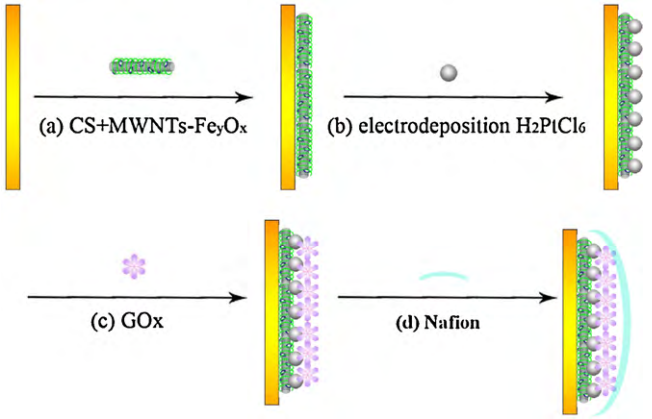

Scheme 1. The stepwise fabrication processes of the modified electrode.

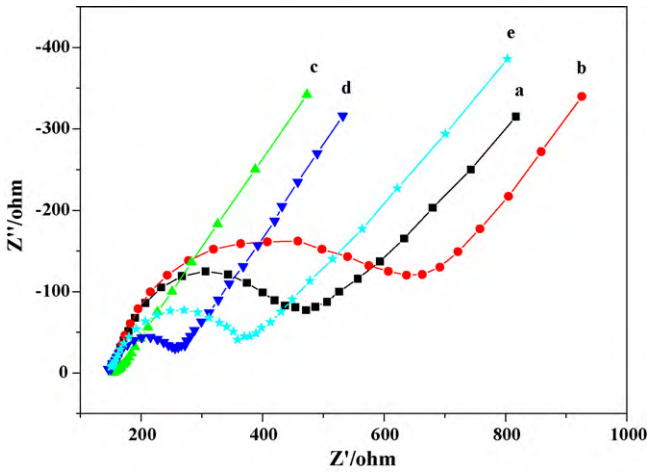

Fig. 2. EIS of the electrode at different stages: (a) bare GCE, (b) Fe_yO_x-MWCNTs/CS/GCE, (c) Pt/Fe_yO_x-MWCNTs/CS/GCE, (d) GOx/Pt/Fe_yO_x-MWCNTs/CS/GCE, (e) Nafion/GOx/Pt/Fe_yO_x-MWCNTs/CS/GCE. Supporting electrolyte: 5 mM $[Fe(CN)_6]^{4-/3-}$ solution.

2 h, and then it was sonicated for 50 min. Finally, the MWCNTs-Fe_yO_x/CS composite was formed.

2.4. Configuration of different modified electrodes

The bare GCE was polished successively with 0.3 and 0.05 μm Al_2O_3 before modification, rinsed with double-distilled water, and sonicated in acetone and double-distilled water for 5 min, respectively.

First, 10 μL of Fe_yO_x-MWCNTs/CS composite was dropped onto the cleaned GCE surface and then dried in air. The Fe_yO_x-MWCNTs/CS/GC obtained was thoroughly rinsed with double-distilled water and then immersed in 5.0 mL 1% H_2PtCl_6 solution for 110 s under the potentials of −0.2 V, to carry out the electrodeposition of Pt nanoparticles. Following that, the fresh solution of GOx (10 mg/mL) was prepared in phosphate buffer solution (PBS, 0.1 M, pH 7.0) and 10 mL solution of freshly prepared GOx was mechanically spread onto the desired Fe_yO_x-MWCNTs/CS/GCE and allowed to dry slowly at 4 °C. At last, these GOx/Fe_yO_x-MWCNTs/CS/GCE bioelectrodes were coated with an extra 2.5 μL layer of 0.5% Nafion. For comparison, the electrode without MWCNTs, and Fe_yO_x were prepared similarly. When these biosensenors were not in use, they were stored at 4 °C in a refrigerator. The fabricated procedure of the biosensor was shown in Scheme 1.

3. Results and discussion

3.1. Characterization of the MWCNTs and Fe_yO_x-MWCNTs composite and evaluation of the electrochemical performance of the glucose biosensor

Fig. 1a is the TEM micrograph of MWCNTs. It can be seen that the MWCNTs shows well-graphitized walls without any remarked coverage with other materials, the diameter of the nanotubes is about 30 nm. Fig. 1b shows a TEM micrograph of a typical iron oxide nanoparticles-decorated MWCNTs. It is found that the iron oxide nanoparticles were attached on the surface of the MWCNTs, and the sizes of the particles ranged from 16 to 28 nm. This feature endows the Fe_yO_x-MWCNTs composites with a high surface area.

EIS of $[Fe(CN)_6]^{4-/3-}$ solution is a valuable and convenient method to give information on impedance changes of the electrode surface in the modification process. In EIS, the semicircle diameter in the impedance spectrum equals the electron-transfer resistance, R_{et}. This resistance controls the electron transfer kinetics of redox probe ($[Fe(CN)_6]^{4-/3-}$) at the electrode interface. It can be seen that a well-defined semicircle curve was obtained with the bare GCE (Fig. 2a). After Fe_yO_x-MWCNTs/CS composite was covered onto the GCE, the diameter of the semicircle increased (Fig. 2b),

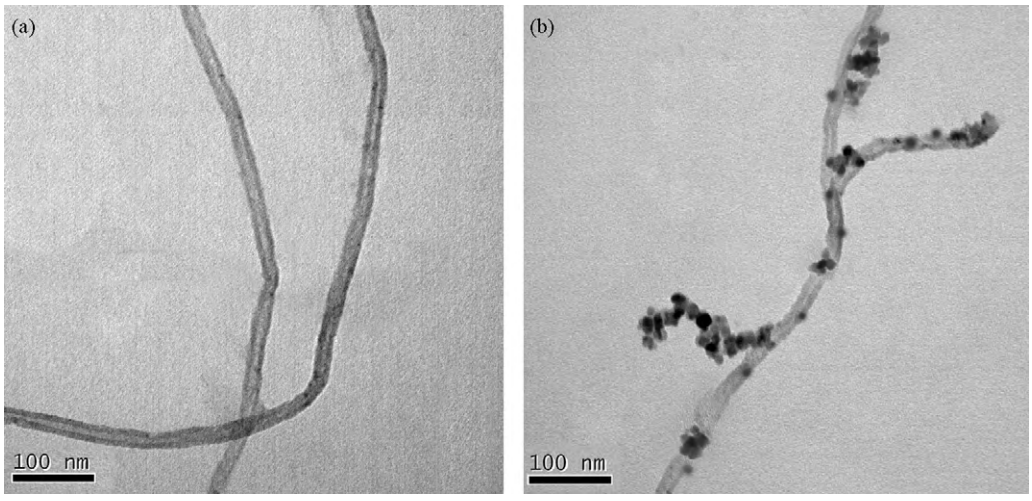

Fig. 1. TEM images of the samples: (a) MWCNTs and (b) Fe_yO_x decorated MWCNTs.

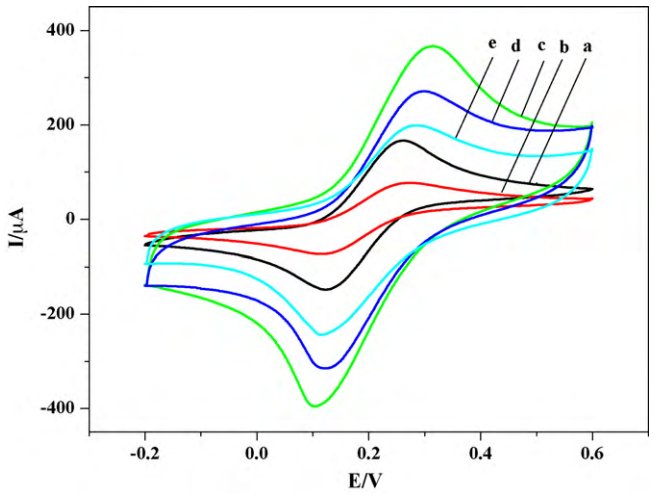

Fig. 3. CV of the electrode at different stages: (a) bare GCE, (b) Fe_yO_x-MWCNTs/CS/GCE, (c) Pt/Fe_yO_x-MWCNTs/CS/GCE, (d) GOx/Pt/Fe_yO_x-MWCNTs/CS/GCE, (e) Nafion/GOx/Pt/Fe_yO_x-MWCNTs/CS/GCE. Supporting electrolyte: 5 mM $[Fe(CN)_6]^{4-/3-}$ solution; scan rate, 50 mV/s.

showing that the composite film blocked the electron transfer of the electrochemical probe. Though Fe_yO_x-MWCNTs composite can increase electron mobility at the electrode surface, the "block effect" induced by non-conductive CS made the diameter of the semicircle increase. When the Pt nanoparticles electrodeposited on the Fe_yO_x-MWCNTs/CS/GCE, a straight line was observed in the EIS of the resulting electrode (Fig. 2c). This may be ascribed to the excellent conductivity of the Pt nanoparticles [32]. With the GOx adsorption on Pt nanoparticles (Fig. 2d), an obvious semicircle domain was obtained, implying an increase of R_{et} of the redox probe on the GOx/Pt/Fe_yO_x-MWCNTs/CS/GCE. This increase is attributed to the non-conductive properties of GOx, which would obstruct electron transfer of the electrochemical probe. At the last step of assembly, Nafion was tied to the GOx (Fig. 2e), R_{et} increased again. This increase is attributed to the non-conductive properties of Nafion, which would obstruct electron transfer of the electrochemical probe. The above results could clearly confirm the success of the assembly of the electrode.

CV is a simple and easy mean to show the changes of electrode behavior after each assembly step, because the electron transfer between the solution species and the electrode must occur by tunneling through either the barrier or the defects in the barrier. Fig. 3 shows the CVs of bare GCE (Fig. 3a), Fe_yO_x-MWCNTs/CS/GCE (Fig. 3b), Pt/Fe_yO_x-MWCNTs/CS/GCE (Fig. 3c), GOx/Pt/Fe_yO_x-MWCNTs/CS/GCE (Fig. 3d) and Nafion/GOx/Pt/Fe_yO_x-MWCNTs/CS/GCE (Fig. 3e) in 5 mM $[Fe(CN)_6]^{4-/3-}$ solution with a scan rate of 50 mV/s. At the bare GCE, well-defined oxidation and reduction peaks of $[Fe(CN)_6]^{4-/3-}$ were observed at 260 mV and 134 mV (Fig. 3a). After the electrode was modified with Fe_yO_x-MWCNTs/CS composite, a large decrease in peak current was observed (Fig. 3b). The decrease was attributed to the non-conductive properties of CS and semiconductive properties of Fe_yO_x. Compared with Fig. 3b, a remarkable peak current increase was observed in Fig. 3c, owing to the Pt nanoparticles which played an important role similarly to a conducting wire or electron conduction tunnel. When the GOx was assemblied on the electrode, the peak current clearly decreased (Fig. 3d), indicating that the non-conductive GOx was incorporated on the Pt/Fe_yO_x-MWCNTs/CS/GCE. A further decrease in peak current is observed (Fig. 3e) after Nafion film was covered onto the electrode. The reason was that Nafion was negatively charged and hindered the diffusion of ferricyanide ion toward the electrode surface. On the basis of the EIS and CV results, we can conclude that GOx is successfully immobilized on the Pt nanoparticles.

3.2. Optimum conditions of the glucose biosensor

In order to obtain an efficient biosensor for determination of glucose, the influence of pH, applied potential and deposition time on the response of the modified electrode were investigated. The change of chronoamperometric current at various pHs ranged from 4.5 to 8.5 under constant glucose concentration (6.0×10^{-5} M) was shown in Fig. 4. It can be seen that the response increased clearly from pH 4.5 to pH 7.0, and reached the maximum at pH 7.0, then the further increase of PBS pH led to decrease of the response (Fig. 4A), indicating that the catalytic response were controlled by the enzymatic activity. So the PBS of pH 7.0 was selected for further experiments.

Fig. 4B shows the dependence of the chronoamperometric current response to constant concentration (6.0×10^{-5} M) glucose on the applied potential in the range from 0 to 0.7 V. Although amperometric current increased gradually when the applied potential shifted from 0 to 0.7 V, an applied potential of 0.3 V was selected for the amperometric determination of glucose. Because we not only could obtain sufficient current responses but also could minimize the risk for interfering reactions of other electroactive species in the solution at 0.3 V.

The effect of deposition time on the chronoamperometric current response was examined from 90 s to 130 s, and the results were shown in Fig. 4C. It can be seen that the response increases sharply from 90 s to 110 s, and reach the maximum at 110 s, then the further increase of deposition time led to roughly decrease of the response (Fig. 4C). The reason was that the decrease of the real surface area of the electrode resulting from the deposition of a large amount of Pt nanoparticles on the electrode surface. Therefore, a deposition time of 110 s was selected for the amperometric determination of glucose.

3.3. Amperometric response of glucose biosensor

We compared the chronoamperometric response of differently modified electrodes with successive injections glucose to a continuous stirring 5 mL PBS under the optimized conditions. As shown in Fig. 5, Nafion/GOx/Pt/Fe_yO_x-MWCNTs/CS/GCE (Fig. 5c) showed the best response to the addition of the same glucose concentration. As controlled experiment, the Nafion/GOx/Pt/MWCNTs/CS/GCE (Fig. 5b) and Nafion/GOx/Pt/Fe_yO_x/CS/GCE (Fig. 5a) exhibited less sensitive amperometric responses to glucose as the lack of Fe_yO_x or MWCNTs. This phenomenon is consistent with the fact that the synergistic action of Fe_yO_x and MWCNTs made the biosensor have excellent electrocatalytic activity. Without the GOx, the Nafion/Pt/Fe_yO_x-MWCNTs/CS/GCE (Fig. 5d) also appeared certain electrochemical catalysis response to glucose, which can be attributed to the inherent catalysis of Pt nanoparticles.

3.4. Chronoamperometric response and calibration curve

Fig. 6 represents the amperometric response curve of the Nafion/GOx/Pt/Fe_yO_x-MWCNTs/CS/GCE under the optimal conditions. The response current increases with increasing concentration of glucose as illustrated in Fig. 6. There is an excellent linear relation of the current with concentration of glucose from 6.0 μM to 6.2 mM, as shown in the lower inset of Fig. 6. The linear regression equation is i (μA) = −7.5 + 13.6 [glucose] (mM) with a correlation coefficient of 0.995. The detection limit can be estimated for 2.0 μM defined from a signal/noise ratio of 3. In addition, the proposed biosensor reached 95% of steady-state current within 15 s.

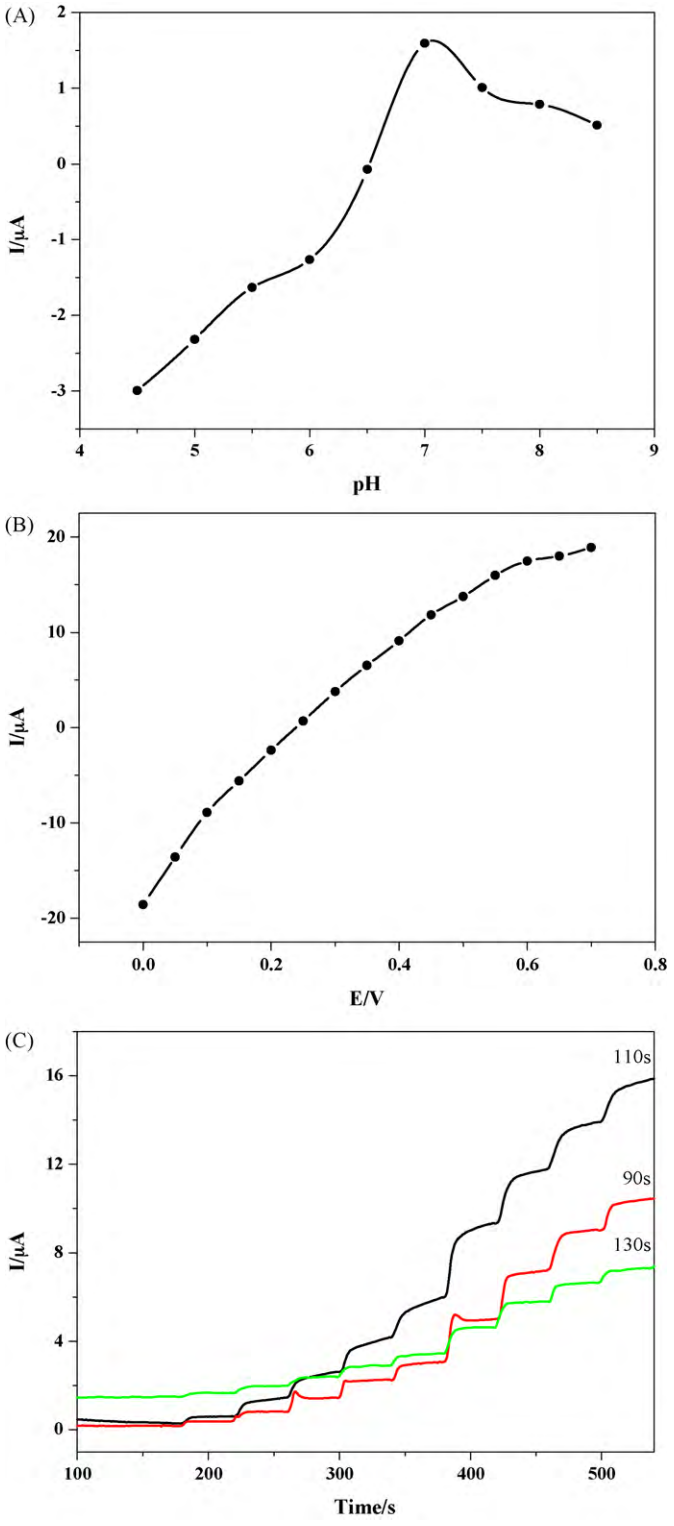

Fig. 4. Dependence of the current response of biosensor to 0.06 mM glucose on the pH of buffer solutions at an applied potential of 0.3 V (A) and on the applied potential in 0.1 M PBS (pH 6.0) (B), the influence of deposition time on the response of the biosensor with successive injection of different concentration of glucose into a stirred solution of 0.1 M PBS (pH 7.0) (C).

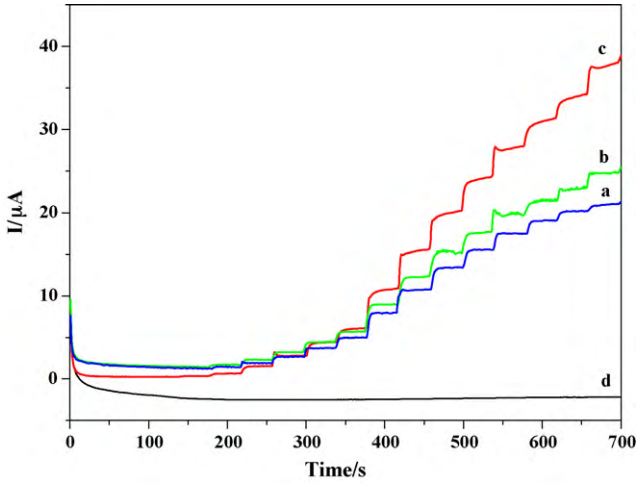

Fig. 5. The chronoamperometry response at applied potential of 0.3 V with successive injection of different concentration of glucose into a stirred solution of 0.1 M PBS (pH 7.0) for Nafion/GOx/Pt/Fe_yO_x/CS/GCE (a), Nafion/GOx/Pt/MWCNTs/CS/GCE (b), Nafion/GOx/Pt/Fe_yO_x-MWCNTs/CS/GCE (c), Nafion/Pt/Fe_yO_x-MWCNTs/CS/GCE (d).

The apparent Michaelis–Menten constant K_M^{app} was generally used to evaluate the biological activity of immobilized enzyme and it could be calculated according to the Michaelis–Menten equation [33]:

$$\frac{1}{I_{ss}} = \frac{1}{I_{max}} + \frac{K_M^{app}}{I_{max}C}.$$

where I_{ss} is the steady-state current after the addition of substrate, C referred to the glucose concentration, and I_{max} is the maximum current measured under saturated substrate conditions and K_M^{app} stands for the apparent Michaelis–Menten constant of the system. The value of the apparent Michaelis–Menten constant (K_M^{app}) can be calculated from the slope (K_M^{app}/I_{max}) and the intercept ($1/I_{max}$) for the plot of the reciprocals of the steady-state current (I_{ss}) versus glucose concentration (C). Thus the K_M^{app} value for the modified electrode was calculated to be 9.0 mM. The low value of K_M^{app} indicates that GOx immobilized in Pt/Fe_yO_x-MWCNTs/CS film retains its bioactivity and has a high biological affinity to glucose. The results were compared with those of other glucose biosensing systems, as shown in Table 1. The comparative data suggest the superior-

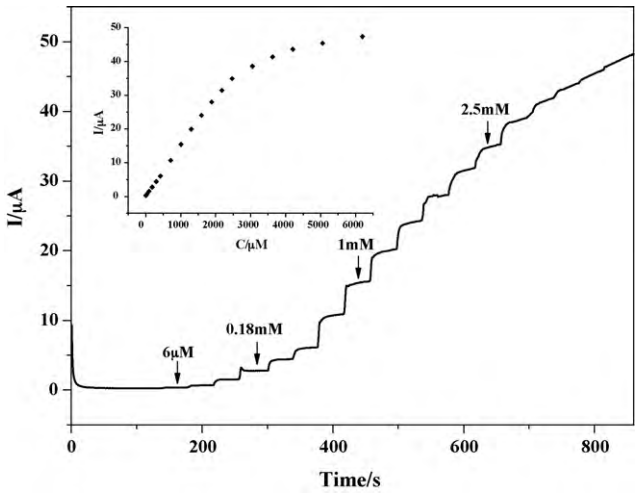

Fig. 6. Typical current–time response of the biosensor on successive injection of different concentration of glucose into a stirred solution of 0.1 M PBS (pH 7.0) at an applied potential of 0.3 V in the time intervals of 40 s. Inset shows linear calibration curves.

Table 1
Comparison of the performance of different glucose biosensors.

Electrode modifier	Linearity (mM)	Detection limit (μM)	K_M^{app} (mM)	Response time (s)	Ref.
CNTs/PtNP/CH-MTOS/GOx	0.0013–6.00	0.3	7.90	5	[34]
Au-CS/Pt/GOx	0.50–16.00	7.0	10.5	8	[35]
ACS-MWCNTs-Pt-GOx	0.05–10.50	6.18	11.02	5	[36]
Ti/TiO_2/Au/PB/GOx	0.015–4.00	5.0	–	10	[37]
CS-Fe_3O_4/GOx	0.50–22.00	50	0.141	5	[16]
Proposed biosensor	0.006–6.20	2.0	9.00	8	Present work

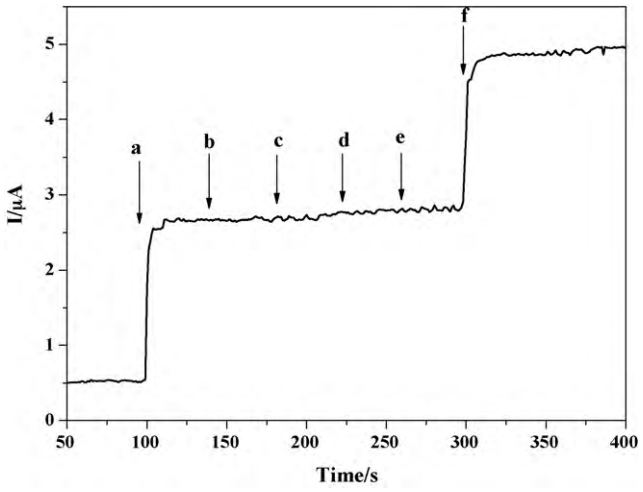

Fig. 7. Effect from the possible interferents in glucose biosensors. The arrows show the each moment at the injection of the interfering compounds: (a) 0.3 mM glucose; (b) 0.9 mM ascorbic acid; (c) 0.9 mM l-cysteine; (d) 0.9 mM threonine; (e) 0.9 mM uric acid; (f) 0.3 mM glucose.

ity of the present biosensor over some earlier reported glucose biosensors, especially the characteristics of linearity range, detection limit, and response time.

3.5. Storage stability of the glucose biosensor

The storage stability of the glucose biosensor was studied in the current work. To evaluate the storage stability of the glucose biosensor, the Nafion/GOx/Pt/Fe_yO_x-MWCNTs/CS modified GCE was stored at 4 °C when not in use. After storage for 1 week, the response of the biosensor was maintained about 91.5% of the initial values. The biosensor still retained 86.8% of its original values for at least 2 weeks. The decreased current may be attributed to the enzymes which partly lose the bioactivity for long storing time.

3.6. Interference determination

Interference studies were performed with the present biosensor in the presence of the selective receptor in a competitive study. Four interfering substances (ascorbic acid, *l*-cysteine, threonine, uric acid) were used to evaluate the selectivity of the biosensor. Amperometric responses were obtained by injection of 0.3 mM glucose and interfering species of different concentration. From the chronoamperometric curve (Fig. 7), we can see that the four tested substances did not significantly interfere with the determination of glucose when the proposed biosensor was employed. This was largely due to the low working potential (about 0.3 V), no electrochemical reactions occurred at this potential.

4. Conclusions

In this work, a novel glucose biosensor was obtained by using the electrodeposition of Pt nanoparticles in Fe_yO_x-MWCNTs/CS composite modified GCE followed by adsorption of GOx at the Pt/Fe_yO_x-MWCNTs/CS composite. Fe_yO_x-MWCNTs act as efficient conduits for electrons and effective supports for Pt nanoparticles. The combination of Fe_yO_x-MWCNTs and Pt nanoparticles in the biosensor results in the improvement of analytical performance, characterized by broader linear range and lower detection limit for glucose determination, as compared to those MWCNTs and Fe_yO_x-based glucose biosensors. The immobilization of GOx at Pt/Fe_yO_x-MWCNTs/CS composite modified GCE by adsorption provides a good microenvironment for GOx and retains its bioactivity. In addition, these composite materials can also conveniently extend to the immobilization of other biomolecules. Such a proposed strategy would be potentially useful for the preparation of other enzyme sensor.

Acknowledgements

This work was supported by the NNSF of China (20675064), the Ministry of Education of China (Project 708073), the Natural Science Foundation of Chongqing City (CSTC-2009BA1003) and High Technology Project Foundation of Southwest University (XSGX02), China.

References

[1] S.R. Lee, Y.T. Lee, K. Sawada, H. Takao, M. Ishida, Biosens. Bioelectron. 24 (2008) 410–414.
[2] J.D. Newman, A.P.F. Turner, Biosens. Bioelectron. 20 (2005) 2435–2453.
[3] X.W. Shen, C.Z. Huang, Y.F. Li, Talanta 72 (2007) 1432–1437.
[4] C. Song, P.E. Pehrsson, W. Zhao, Materials Research society, J. Mater. Res. 21 (2006) 2817–2823.
[5] Z. Cheng, E. Wang, X. Yang, Biosens. Bioelectron. 16 (2001) 179–185.
[6] X.M. Chen, Z.M. Cai, Z.J. Lin, T.T. Jia, H.Z. Liu, Y.Q. Jiang, X. Chen, Biosens. Bioelectron. 24 (2009) 3475–3480.
[7] M. Morikawa, N. Kimizuka, M. Yoshihara, T. Endo, Chem. Eur. J. 8 (2002) 5580–5584.
[8] J. Wang, D.F. Thomas, A. Chen, Anal. Chem. 80 (2008) 997–1004.
[9] Y.Y. Song, D. Zhang, X.H. Xia, Chem. Eur. J. 11 (2005) 2177–2182.
[10] Y.Z. Xian, Y. Hu, F. Liu, Y. Xian, L.J. Feng, L.T. Jin, Biosens Bioelectron. 22 (2007) 2827–2833.
[11] O.A. Raitman, E. Katz, A.F. Buckmann, I. Willner, J. Am. Chem. Soc. 124 (2002) 6487–6496.
[12] M. Yang, Y. Yang, Y. Liu, G. Shen, R. Yu, Biosens. Bioelectron. 21 (2006) 1125–1131.
[13] M. Yang, Y. Yang, H. Yang, G. Shen, R. Yu, Biomaterial 27 (2006) 246–255.
[14] H. Yang, T.D. Chung, Y.T. Kim, C.A. Choi, C.H. Jun, H.C. Kim, Biosens. Bioelectron. 17 (2002) 251–259.
[15] T. Tanaka, T. Matsunaga, Anal. Chem. 72 (2000) 3518–3522.
[16] K. Ajeet, K. Raju, R.S. Pratima, P. Pratibha, A. Javed, A. Sharif, B.D. Malhotra, Biosens. Bioelectron. 24 (2008) 676–683.
[17] D.F. Cao, P.L. He, N.F. Hu, Analyst 128 (2003) 1268–1274.
[18] S.H. Lim, J. Wei, J.Y. Lin, Q.T. Li, J.K. You, Biosens. Bioelectron. 20 (2005) 2341–2346.
[19] S.G. Wang, Q. Zhang, R. Wang, S.F. Yoon, J. Ahn, D.J. Yang, J.Z. Tian, J.Q. Li, Q. Zhou, Electrochem. Commun. 5 (2003) 800–803.
[20] J. Wang, M. Musameh, Y. Lin, J. Am. Chem. Soc. 125 (2003) 2408.
[21] J. Wang, M. Li, Z. Shi, N. Li, Z. Gu, Anal. Chem. 74 (2002) 1993.
[22] X.Y. Pang, D.M. He, S.L. Luo, Q.Y. Cai, Sens. Actuators B 137 (2009) 134–138.
[23] R.B. Rakhi, K. Sethupathi, S. Ramaprabhu, J. Phys. Chem. B 13 (2009) 3190–3194.
[24] P.C.P. Watts, W.K. Hsu, D.P. Randall, V. Kotzeva, G.Z. Chen, Chem. Mater. 14 (2002) 4505.

[25] Y.H. Wu, P.W. Qiao, J.J. Qiu, T.C. Chong, T.S. Low, Nano Lett. 2 (2002) 161–164.
[26] G. Vasilios, T. Vasilios, G. Dimitrios, P. Dimitrios, Chem. Mater. 17 (2005) 1613.
[27] S.C. Tsang, Y.K. Chen, P.J.F. Harris, M.L.H. Green, Nature 372 (1994) 159–162.
[28] B.K. Pradhan, T. Toba, T. Kyotani, A. Tomita, Chem. Mater. 10 (1998) 2510–2515.
[29] Y.X. Cheng, Y.J. Liu, J.J. Huang, K. Li, Y.Z. Xian, W. Zhang, L.T. Jin, Electrochim. Acta 54 (2009) 2588–2594.
[30] M.L. Guo, J.H. Chen, L.H. Nie, S.Z. Yao, Electrochim. Acta 49 (2004) 2637–2643.
[31] C.L. Chen, J. Hu, D.D. Shao, J.X. Li, X.K. Wang, J. Hazard. Mater. 64 (2009) 923–928.
[32] X.H. Kang, Z.B. Mai, X.Y. Zou, P.X. Cai, J.Y. Mo, Anal. Biochem. 369 (2007) 71–79.
[33] R.A. Kamin, G.S. Willson, Anal. Chem. 52 (1980) 1198–1205.
[34] X. Kang, Z. Mai, X. Zou, P. Cai, J. Mo, Talanta 74 (2008) 879–886.
[35] B.Y. Wu, S.H. Hou, F. Yin, J. Li, Z.X. Zhao, J.D. Huang, Q. Chen, Biosens. Bioelectron. 22 (2007) 838–844.
[36] M.C. Tsai, Y.C. Tsai, Sens. Actuators B 141 (2009) 592–598.
[37] P. Benvenuto, A.K.M. Kafi, A.C. Chen, J. Electroanal. Chem. 627 (2009) 76–81.